Simultaneous empirical interpolation and reduced basis method. Application to non-linear multi-physics problem

Cécile Daversin, Christophe Prud'Homme

Simultaneous empirical interpolation and reduced basis method. Application to non-linear multi-physics problem.

Cécile Daversin and Christophe Prud'homme

Abstract This paper focuses on the reduced basis method in the case of non-linear and non-affinely parametrized partial differential equations where affine decomposition is not obtained. In this context, Empirical Interpolation Method (EIM) [4] is commonly used to recover the affine decomposition necessary to deploy the Reduced Basis (RB) methodology. The build of each EIM approximation requires many finite element solves which increases significantly the computational cost hence making it inefficient on large problems [5]. We propose a Simultaneous EIM and RB method (SER) whose principle is based on the use of reduced basis approximations into the EIM building step. The number of finite element solves required by SER can drop to $N+1$ where N is the dimension of the RB approximation space, thus providing a huge computational gain. The SER method has already been introduced in [1] through which it is illustrated on a 2D benchmark itself introduced in [3]. This paper develops the SER method with some variants and in particular a multilevel SER, SER(ℓ) which improves significantly SER at the cost of $\ell N+1$ finite element solves. Finally we discuss these extensions on a 3D multi-physics problem.

1 Introduction

The demand in terms of real time simulations and uncertainty quantification is fast growing area in engineering, together with the size and the complexity of the considered problems. Reduced order methods, and in particular the reduced basis methods, play a critical role at breaking complexity.

Especially designed for real-time and many-query simulations, the Reduced Basis (RB) method offers an efficient evaluation of quantities of interest and covers a large range of problems among which non-affinely parametrized Partial Differential Equations (PDE). Based on the so-called offline/online decomposition, this method distinguishes the parameter independent terms whose computation is costly due to their dependence on the finite element dimension. Allowing to compute the latter only once, such a decomposition is not necessarily available in particular for non-affine/non-linear problems. The Empirical Interpolation Method (EIM) is classically used prior to the RB methodology to recover an affinely parametrized problem ensuring the availability of the offline/online decomposition. We proposed a simultaneous EIM-RB (SER) method [1] to circumvent the possibly dissuasive additional cost required by the EIM buidling step. Building together the affine decomposition as well as the RB approximation space, SER indeed requires only but a few finite elements solves.

Following up [1], this paper reports a finer analysis of SER and its variants along with its expanded use to non-linear multi-physics problem. In particular we introduce a multilevel SER, SER(ℓ) which improves significantly SER. After a reminder of the SER method in the context of non-affinely parametrized PDEs, we first give an overview of the

Cécile Daversin
IRMA, 7 rue René Descartes, 67084 Strasbourg cedex, France, e-mail: daversin@math.unistra.fr

Christophe Prud'homme
IRMA, 7 rue René Descartes, 67084 Strasbourg cedex, France, e-mail: prudhomme@unistra.fr

investigated variants. All of them are based on the development of an error indicator initially designed to guide the construction of the RB approximation space from a Greedy algorithm. The second part illustrates these variants with results obtained on a benchmark introduced in [3] on which the SER preliminary results shown in [1] were based. The last part focuses on the application of SER and SER(ℓ) to a non-linear multi-physics problem from the HiFiMagnet project aiming to design an efficient model for high field magnets [2].

2 A simultaneous EIM-RB method

Let $u(\mu)$ be the solution of a non-linear and non-affinely parametrized PDE, where μ denotes the p-vector of inputs defined in the parameter space $\mathscr{D} \subset \mathbb{R}^p$. The non-affine parametrization comes from the dependance of the PDE on at least one non-affine function $w(u(\mu),x;\mu)$. Considering $X \subset H^1(\Omega)$ an Hilbert space whose scalar product is denoted as $(\cdot,\cdot)_X$, the variational formulation of the PDE consists in finding $u(\mu) \in X$ as a root of a functional r such that

$$r(u(\mu),v;\mu;w(u(\mu),x;\mu)) = 0 \; \forall v \in X. \tag{1}$$

2.1 Preliminaries

We denote by $X^{\mathscr{N}} \subset X$ the finite element approximation space of dimension $\mathscr{N}$ in which the approximation $u_{\mathscr{N}}(\mu)$ of $u(\mu)$ resides. The non linearity of the considered PDE is handled through iterative methods. The following description relies on a Newton algorithm for which we introduce j the Jacobian associated with the functional r of (1), and ${}^k u(\mu)$ the solution at k-th Newton's iteration. The problem (1) then consists in finding $\delta^{k+1}u(\mu) \equiv {}^{k+1}u(\mu) - {}^k u(\mu) \in X^{\mathscr{N}}$ such that

$$j(u,v;\mu;{}^k u(\mu);w({}^k u(\mu),x;\mu))\delta^{k+1}u(\mu) = -r({}^k u(\mu),v;\mu;w({}^k u(\mu),x;\mu)) \tag{2}$$

2.1.1 Empirical interpolation method

As previously mentionned, the reduced basis method is based on an offline/online strategy assuming the existence of an affine decomposition of (2). The dependance of j and r on $w(u(\mu),x;\mu)$ stands in the way of the availability of such decomposition. In this context, the Empirical Interpolation method (EIM) is widely used to recover an affinely parametrized problem from (2) building an affine approximation $w_M(u(\mu),x;\mu)$ of $w(u(\mu),x;\mu)$ reading as

$$w_M(u(\mu),x;\mu) = \sum_{m=1}^{M} \beta_m^M(u(\mu);\mu) q_m(x) \tag{3}$$

whose approximation coefficients β_m^M results from the resolution of a $M \times M$ system ensuring the exactness of w_M at a set of interpolation points $\{t_i\}_{i=1}^M$.

To this end, we first introduce a subset Ξ of $\mathscr{D}$ from which a sample $\bar{S}_M = \{\bar{\mu}_1,\ldots,\bar{\mu}_M\} \in \mathscr{D}^M$ is built. The EIM approximation space $\bar{W}_M = span\{\bar{\xi}_m \equiv w(u(\bar{\mu}_m),x;\bar{\mu}_m), 1 \leqslant m \leqslant M\}$ in which the approximation $w_M(u(\mu),x;\mu)$ shall reside consists of the set of w evaluations on $\bar{S}_M$ elements. As starting point of the EIM algorithm, the first sample point $\bar{\mu}_1$ is picked in Ξ assuming $\bar{\xi}_1 \neq 0$.

$$\bar{\xi}_1 = w(u(\bar{\mu}_1),x;\bar{\mu}_1), \quad t_1 = arg\sup_{x\in\Omega} |\bar{\xi}_1(x)|, \quad q_1 = \frac{\bar{\xi}_1(x)}{\bar{\xi}_1(t_1)} \tag{4}$$

The next sample points $\{\bar{\mu}_m\}_{m=2}^M$ are then selected through a Greedy algorithm as

$$\bar{\mu}_M = arg\max_{\mu\in\Xi} \inf_{z\in W_{M-1}} ||w(.;.;\mu) - z||_{L^\infty(\Omega)} \tag{5}$$

leading to the EIM approximation space enrichment $\bar{W}_M = \bar{W}_{M-1} \oplus span\{\xi_M\}$. The computation of the coefficients $\beta_m^{M-1}(u(\bar{\mu}_M);\bar{\mu}_M)$ allows to evaluate the residual $r_M(x) = w(u(\bar{\mu}_M),x;\bar{\mu}_M) - w_{M-1}(u(\bar{\mu}_M),x;\bar{\mu}_M)$ defining the interpolation point t_M and the next basis function q_M as

$$t_M = arg\sup_{x\in\Omega} |r_M(x)|, \quad q_M(x) = \frac{r_M(x)}{r_M(t_M)} \tag{6}$$

2.1.2 Reduced basis method

Defined as the linear combination of the finite element solutions forming the RB approximation space $W_N = \{\xi_n\}_{i=1}^N$, the reduced basis approximation $u_N(\mu)$ of $u(\mu)$ reads as

$$u_N(\mu) = \sum_{i=1}^{N} u_{N,i}(\mu)\xi_i \tag{7}$$

Based on a sample $S_N = \{\mu_1,\cdots,\mu_N\} \subset \mathscr{D}$ with $N << \mathscr{N}$, W_N is built from the set of finite element solutions $\{u_{\mathscr{N}}(\mu_i)\}_{i=1}^N$ which are orthonormalized, with respect to the scalar product of X, through a Gram-Schmidt algorithm. As $u_{\mathscr{N}}(\mu)$, the reduced basis approximation $u_N(\mu)$ has to satisfy the equation (1). The computation the $u_{N,j}$ in the RB approximation space W_N consists in solving the $N\times N$ reduced system (8) considering $\{\xi_n\}_{i=1}^N$ as test functions

$$\sum_{j=1}^{N} j(\xi_j,\xi_l;\mu;{}^k u_N; w({}^k u_N,x;\mu))\delta^{k+1}u_{N,j} - r(\xi_l;\mu;{}^k u_N; w({}^k u_N,x;\mu)) \tag{8}$$

where $\delta^{k+1}u_{N,j} \equiv ({}^{k+1}u_{N,j} - {}^k u_{N,j})$ and with $1 \leqslant j,l \leqslant N$.

2.2 SER *method*

Offering both an efficient computation of W_N and an efficient assembly of the reduced system (8) by means of the precomputation of the parameter independent terms of (2), the affine decomposition obtained through the EIM approximation of $w(u(\mu),x;\mu)$ is a core enabler of the reduced basis method. The initialization step (4) requires one finite element solve which is unavoidable, subsequently the finite element solves are needed by the Greedy algorithm (5) and the complexity scales with the size of the EIM trainset Ξ. The EIM offline step has a prohibitive cost.

Introduced in [1], the simultaneous EIM-RB (SER) method reduces this cost using the readily available reduced approximation into the Greedy algorithm instead of finite element solves. Due to the lack of reduced approximation at the initialization step (4) and as mentioned previously, the finite element solve of the full non-linear problem (2) for the first EIM approximation w_1 cannot be avoided. (2) is never solved afterwards. This leads to a first rough affine decomposition making the reduced basis methodology feasible, and it results in a first reduced approximation to be used in the EIM Greedy algorithm (5). From there, EIM and RB approximations spaces are enriched alternately using solely RB approximations making the number of finite element solves required drop to one for the EIM offline step.

The parameter selection process is then based on the last reduced basis approximation u_{M-1}

$$\bar{\mu}_M = arg\max_{\mu\in\Xi} \inf_{z\in W_{M-1}} ||w(u_{M-1}(\mu);.;\mu) - z||_{L^\infty(\Omega)} \tag{9}$$

used as well to build the current EIM basis function

$$\bar{\xi}_M = w(u_{M-1}(\bar{\mu}_M); x; \bar{\mu}_M)\,. \tag{10}$$

The residual $r_M(x) = w(u_{M-1}(\bar{\mu}_M), x; \bar{\mu}_M) - w_{M-1}(u_{M-1}(\bar{\mu}_M), x; \bar{\mu}_M)$ is also computed from u_{M-1} giving t_M and q_M from (6).

2.2.1 Error estimation

The Greedy algorithm used in the EIM offline step – either based on finite element solve (5) or on reduced basis approximation (14) – rests on the maximum value of a functional related with the approximation error. In the absence of such an error indicator, the RB sample S_N on which the RB approximation space is based is built from a random selection process. This is the case for the preliminary results displayed in [1]. In order to improve the reliability of the reduced basis approximation, we build W_N from a Greedy algorithm based on an error indicator. In the context of SER, this should improve the quality of the reduced basis approximation used in the EIM algorithm and then the affine decomposition especially during the first steps of SER.

The definition of an error bound for non-linear but affinely parametrized problems is given in [6], based on the norm of the Riesz representation $\mathscr{Y}_r$ of the residual r such that

$$(\mathscr{Y}_r, v)_X = r(v) \tag{11}$$

The definition of such an error bound is not readily feasible for non-linear non affinely parametrized problems. Let us now introduce $r^{aff}_{N,M}$ as the evaluation of (1) from the reduced basis approximation u_N and the EIM approximation w_M which served to build it.

$$r^{aff}_{N,M}(\mu) = r(u_N(\mu), v; \mu; w_M(u(\mu), x; \mu)) \tag{12}$$

Inspired from [6] but not providing an error bound, the norm of the Riesz representation $\mathscr{Y}^{aff}_{r^{aff}_{N,M}}$ (11) of $r^{aff}_{N,M}$ (12) provides an error indicator. We then use this indicator to drive construction of S_N in the Greedy algorithm

$$\mu_i = arg\ max_{\mu\in\mathscr{D}} \parallel \mathscr{Y}^{aff}_{r^{aff}_{N,M}}(\cdot;\mu) \parallel_X \tag{13}$$

2.2.2 Some SER variants

Besides its use in the S_N building process (13) consisting in a first SER variant, the previously introduced error indicator serves as a quantifier of the reduced basis approximation accuracy through the SER offline procedure. Various alternatives based on this error indicator have been investigated, whose most relevant ones are detailed in the following. They are still illustrated from the results obtained on the 2D benchmark introduced in [3].

r-adaptation

We remind that the SER methodology consists of the simultaneous enrichment of EIM and RB approximation spaces whose basis functions are alternately built one by one. A first alternative consists in changing the frequency of the affine decomposition updates, corresponding to perform the alternate build per groups of size r. In this context, $r = 1$ corresponds to the initial SER method while $r = M$ stands for the standard RB methodology. Intermediary stages with $1 < r < M$ were investigated in [1] with r constant for the whole offline step.

The error indicators come to a criterion providing guidance to perform a smart adaptation of r during the SER process introduced as *r*-adaptation method. As mentionned, the Greedy algorithm used both in EIM (14) and RB (13) offline stage selects the maximizer of a functional given as an indicator of the approximation error. The *r*-adaptation method rests on the increment of the corresponding maximum value between two updates. As a quantifier of the gain in

term of accuracy, the resulting criterion aims to continue the enrichment until a relevant decrease of the approximation error. This adaptation process distinguishes the update frequency of EIM and RB approximation spaces which are considered independently each with their own criterion.

Hybrid Greedy algorithm

As mentionned, the accuracy of the reduced basis approximation plays a key role in the $\bar{S}_M$ building step especially for the first EIM basis functions. Indeed, a reduced basis approximation of poor quality could damage the EIM approximation and consequently the quality of the affine decomposition. In this context, we propose to assess the quality of the reduced basis approximation from the error indicator used in (13) for each parameter of the trainset. In this way, the reduced basis approximation is employed solely on parameters for which it is sufficiently relevant. A parametric finite element solve based on the current affine decomposition is used for the remaining parameters to benefit from the precomputations while considering the whole trainset all through the SER offline step. This leads to an hybrid method combining the use of finite element (14) and RB approximations (5) within the EIM Greedy algorithm.

Multilevel SER(ℓ)

The last variant we propose rests on the application of the SER methodology several times during the offline step. The first level exactly corresponds to the previously introduced SER method whose Greedy algorithm employed for EIM is described in (14). Once the EIM and RB approximation spaces completed, the multilevel SER method consists of restarting the algorithm while benefiting from the reduced basis approximation coming from the previous level. Considering u_N^ℓ the reduced basis approximation obtained at the ℓ-th level, the EIM Greedy algorithm becomes

$$\bar{\mu}_M = arg\max_{\mu\in\Xi} \inf_{z\in W_{M-1}} ||w(u_N^{\ell-1}(\mu);.;\mu) - z||_{L^\infty(\Omega)} \tag{14}$$

Coming from the whole W_N approximation space, the reduced basis approximations used in the EIM Greedy algorithm from the second level offer EIM approximations of better quality. Based on this consideration, the resulting reduced basis approximations are expected to be more accurate as well.

3 Numerical experiments

Based on the 2D non-linear and non affinely parametrized benchmark of [3], the following numerical experiments illustrate the proposed SER variants. We consider the $2D$ domain $\Omega =]0,1[^2$ and the parameter space $\mathscr{D} = [0.01, 10]^2$, this problem consists in finding u such that

$$-\Delta u + \mu_1 \frac{e^{\mu_2 u} - 1}{\mu_2} = 100\sin(2\pi x)\sin(2\pi y) \text{ in } \Omega \text{ with } \mu = (\mu_1, \mu_2) \in \mathscr{D} \tag{15}$$

The non-affinely parametrization of the problem (15) resides in the function $g(u,x;\mu) = \mu_1 \frac{e^{\mu_2 u}-1}{\mu_2}$. Based on a training set $\Xi \subset \mathscr{D}$ of size 225, its EIM approximation $g_M = \sum_{i=1}^{M} \beta_m^M(u,\mu) q_m(x)$ allows to recover the required affine decomposition. Let's consider the absolute error on the solution u and on the output s defined as the average of u over Ω

$$\varepsilon_{M,N}^u = \| u_{\mathscr{N}} - u_N \|_{L_2} \quad \varepsilon_{M,N}^s = | s_{\mathscr{N}} - s_N | \tag{16}$$

where $\cdot_{\mathscr{N}}$ is the finite element solution/output of the initial problem (1) and $\cdot_N$ the reduced basis solution/output.

The following tables display the maximum of the absolute errors (16) obtained on a set a 1000 realizations selected randomly in $\mathscr{D}$. The table 1b reproduces the results in [3] using the standard method with an RB approximation space built from (13), confirming the relevance of the proposed error indicator.

N	M	$\max(\varepsilon^u_{M,N})$	$\max(\varepsilon^s_{M,N})$
5	5	8.37e-3	6.33e-3
10	10	4.33e-4	2.10e-4
15	15	2.60e-4	1.44e-4
20	20	9.14e-5	4.69e-5
25	25	4.18e-5	1.15e-5

(a) Standard - RB Random

N	M	$\max(\varepsilon^u_{M,N})$	$\max(\varepsilon^s_{M,N})$
5	5	8.22e-3	6.27e-3
10	10	2.87e-4	2.09e-4
15	15	1.96e-5	1.47e-5
20	20	1.57e-5	1.32e-5
25	25	3.14e-6	2.52e-6

(b) Standard - RB Greedy

Regarding the SER method, the table 2a displays the results coming from the use of a random selection process within the construction of the RB approximation space while the table 2b illustrates the use of a Greedy algorithm in this context. Although slightly higher than the errors obtained in table 1b, these errors come close the ones obtained in table 1a for a reduced computational cost. Nevertheless, the impact of the previously introduced error indicator on this application turns out to be limited.

N	M	$\max(\varepsilon^u_{M,N})$	$\max(\varepsilon^s_{M,N})$
5	5	1.06e-2	8.23e-3
10	10	2.13e-3	1.6e-3
15	15	5.12e-4	4.22e-4
20	20	3.58e-5	2.27e-5
25	25	2.24e-5	1.44e-5

(a) RB Random

N	M	$\max(\varepsilon^u_{M,N})$	$\max(\varepsilon^s_{M,N})$
5	5	1.04e-2	8.09e-3
10	10	2.40e-3	1.87e-3
15	15	2.38e-4	2.01e-4
20	20	3.02e-5	1.67e-5
25	25	2.65e-5	1.94e-5

(b) RB Greedy

Table 2: Use of Greedy algorithm for RB within SER

The tables 3a and 3b combine the previous Greedy algorithm used to build the RB approximation space with the first two SER variants. The table 3a focus on the $r-$adaptation method while the table 3b investigates the previously introduced ranking of parameters depending on the reduced basis approximation reliability within the EIM Greedy algorithm. Compared to previous SER results displayed in table 2, neither of these variants results in a significative improvement in the error. A similar behaviour is observed combining these two variants.

N	M	$\max(\varepsilon^u_{M,N})$	$\max(\varepsilon^s_{M,N})$
5	5	1.04e-2	8.09e-3
10	10	2.40e-3	1.87e-3
15	15	2.34e-4	1.95e-4
20	20	3.46e-5	2.01e-5
25	25	1.61e-5	9.19e-6

(a) $r-$adaptation (EIM=20%, RB=20%)

N	M	$\max(\varepsilon^u_{M,N})$	$\max(\varepsilon^s_{M,N})$
5	5	1.03e-2	8.06e-3
10	10	2.29e-3	1.77e-3
15	15	2.25e-4	1.87e-4
20	20	3.08e-5	1.77e-5
25	25	1.95e-5	1.40e-5

(b) hybrid EIM (tol = 20%)

Table 3: SER variants based on error indicator

The tables 4a to 4d display the results obtained with the multilevel SER(ℓ)) method. As expected, the results coming from the first level (table 4a) are similar to ones of table 2a. The observed disparity comes from the random selection process performed at RB offline stage which could result in a slightly different RB approximation space.

From the second level illustrated by table 4b, we observe a significant decrease of the error which comes up to the standard case introduced in table 1a. However, the error is no longer visibly evolving at the next levels as shown in tables 4c and 4d.

N	M	$\max(\varepsilon^u_{M,N})$	$\max(\varepsilon^s_{M,N})$
5	5	1.06e-2	8.40e-3
10	10	2.33e-3	1.72e-3
15	15	6.51e-4	5.12e-4
20	20	2.32e-4	1.94e-4
25	25	7.08e-5	5.64e-5

(a) SER(1)

N	M	$\max(\varepsilon^u_{M,N})$	$\max(\varepsilon^s_{M,N})$
5	5	9.13e-3	7.12e-3
10	10	3.19e-4	1.12e-4
15	15	7.56e-5	5.36e-5
20	20	1.54e-4	2.67e-5
25	25	3.52e-5	2.76e-5

(b) SER(2)

N	M	$\max(\varepsilon^u_{M,N})$	$\max(\varepsilon^s_{M,N})$
5	5	7.26e-3	5.58e-3
10	10	2.00e-3	1.13e-3
15	15	5.50e-4	4.43e-4
20	20	2.08e-4	3.27e-5
25	25	1.37e-5	6.87e-6

(c) SER(3)

N	M	$\max(\varepsilon^u_{M,N})$	$\max(\varepsilon^s_{M,N})$
5	5	8.67e-3	6.58e-3
10	10	5.07e-3	3.35e-3
15	15	2.78e-4	2.30e-4
20	20	2.67e-4	4.35e-5
25	25	5.62e-6	2.56e-6

(d) SER(4)

Table 4: SER multilevel - Random

As to the results obtained with SER multilevel method combined with the use of the previous error indicator through a Greedy algorithm within the RB offline stage, they are illustrated in tables 5a to 5d. Their analysis results in the same conclusion as for table 4.

N	M	$\max(\varepsilon^u_{M,N})$	$\max(\varepsilon^s_{M,N})$
5	5	1.04e-2	8.09e-3
10	10	2.39e-3	1.86e-3
15	15	2.38e-4	2.00e-4
20	20	3.03e-5	1.65e-5
25	25	3.42e-5	2.45e-5

(a) SER(1)

N	M	$\max(\varepsilon^u_{M,N})$	$\max(\varepsilon^s_{M,N})$
5	5	9.17e-3	6.99e-3
10	10	2.89e-4	2.07e-4
15	15	4.12e-5	1.87e-5
20	20	1.44e-5	7.61e-6
25	25	2.72e-5	2.20e-5

(b) SER(2)

N	M	$\max(\varepsilon^u_{M,N})$	$\max(\varepsilon^s_{M,N})$
5	5	7.93e-3	6.01e-3
10	10	2.99e-4	1.80e-4
15	15	1.75e-4	1.35e-4
20	20	1.69e-5	6.02e-6
25	25	7.86e-6	5.37e-6

(c) SER(3)

N	M	$\max(\varepsilon^u_{M,N})$	$\max(\varepsilon^s_{M,N})$
5	5	8.46e-3	6.36e-3
10	10	4.34e-4	2.24e-4
15	15	6.28e-5	5.05e-5
20	20	1.76e-5	1.17e-5
25	25	1.92e-5	1.51e-5

(d) SER(4)

Table 5: SER multilevel - RB Greedy

The previous analysis is supported by the convergence study of the considered EIM approximation illustrated in figure 1. The graph of figure 1 plots the maximal value of the functional used in the EIM Greedy algorithm depending on the number of basis functions which compose the EIM approximation space. Compared with the EIM convergence obtained using the standard RB methodology, we can indeed notice a significant error decrease from the second level. The next levels remains comparable to the latter, already very close to the EIM approximation performed from the

standard method.

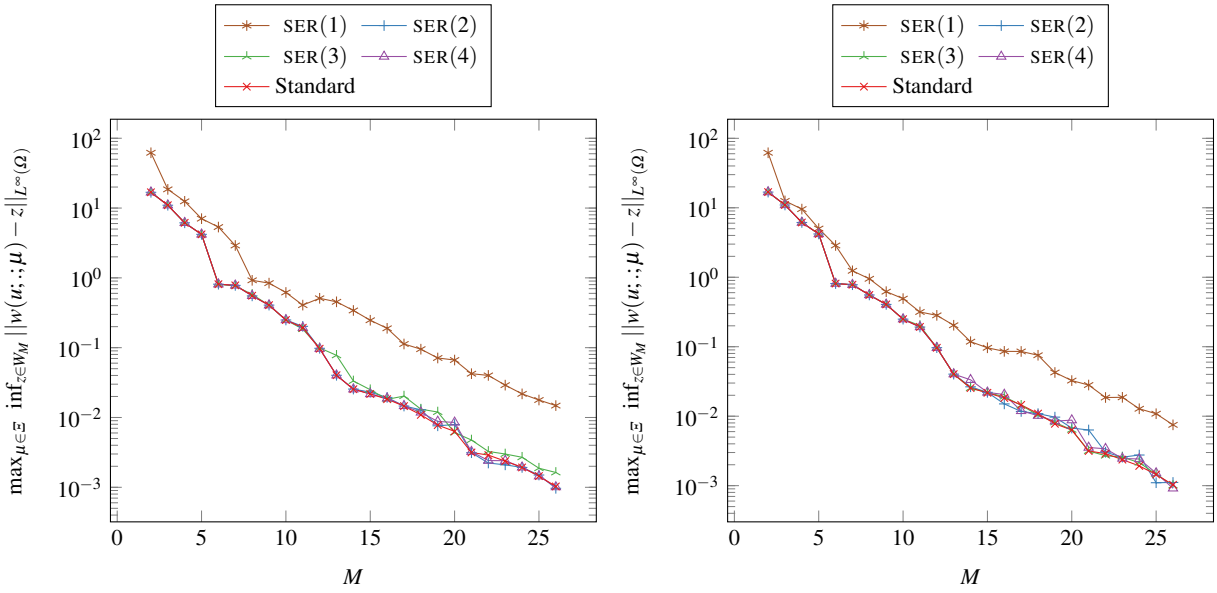

(a) Random

(b) RB Greedy

Fig. 1: SER multilevel - EIM convergence

4 Application to multi-physics model

The HiFiMagnet project [2] aims at developing an efficient multi-physics model for high field magnets. We investigate the pertinence of the SER method on a 3D non-linear electro-thermal model. Considering the multilevel variant which has just been introduced, the initial SER method is denoted as SER(1) in the following.

4.1 Electro-thermal model

The considered electro-thermal model consists of the coupling of the electrical potential V in the magnet with the resulting temperature T. Thus, the temperature T is the solution of the non-linear coupled and non affinely parametrized thermo-electric problem

$$\begin{cases} -\nabla\cdot(\sigma(T)\nabla V) = 0 \\ -\nabla\cdot(k(T)\nabla T) = \sigma(T)\nabla V\cdot\nabla V \end{cases} \tag{17}$$

The non-linearity of (17) is coming from the dependance of the electrical (resp. thermal) conductivity $\sigma(T)$ (resp. $k(T)$) on temperature as well as the joule effect terms

$$\sigma(T) = \frac{\sigma_0}{1+\alpha(T-T_0)} \quad \text{and} \quad k(T) = \sigma(T)LT \tag{18}$$

The temperature coefficient α and the Lorentz number L are proper to the material, and σ_0 represents the electric conductivity at reference temperature $T = T_0$. Related to the current density j in the magnet, the current flow is modeled

from a difference of electrical potential V_D between the current input and the current output imposed as Dirichlet boundary conditions. Other boundaries are considered as electrically insulated through a homogeneous Neumann condition.

$$\begin{cases} V = 0 \text{ on input}, V = V_D \text{ on output} \\ -\sigma(T)\nabla V \cdot \mathbf{n} = 0 \text{ on other boundaries} \end{cases} \tag{19}$$

The temperature increase due to the Joule effect is controled with a water cooling of the magnet corresponding to a forced convection condition on the concerned regions, based on the water temperature T_w and on heat transfer coefficient h.

$$\begin{cases} -k(T)\nabla T \cdot \mathbf{n} = h(T - T_w) \text{ on cooled surfaces} \\ -k(T)\nabla T \cdot \mathbf{n} = 0 \text{ on other boundaries} \end{cases} \tag{20}$$

The input parameter $\mu = (\sigma_0, \alpha, L, j, h, Tw) \in \mathbb{R}^6$ combines material properties and operating conditions parameters, while the considered output is the mean temperature over the magnet acting as a critical parameter in terms of magnet design. The definition of $\sigma(T)$ (18) from the input parameters thus makes the model (17) non-affinely parametrized as well as non-linear. The SER methodology readily applies in this context.

4.2 Application to Bitter magnet

The first application focuses on the geometry illustrated in figure 2 whose mesh is composed of 15388 nodes. This geometry stands for a sector of a Bitter magnet commonly used in the context of high field magnet facilities. The ranges considered for the input parameter given in table 6 are chosen from physical considerations coming both from litterature and experimental measures.

Input	Range
σ_0	$[40 \times 10^6, 60 \times 10^6]\ S.m^{-1}$
α	$[3.3 \times 10^{-3}, 3.5 \times 10^{-3}]\ K^{-1}$
L	$[2.5 \times 10^{-8}, 2.9 \times 10^{-8}]$
j	$[30 \times 10^6, 60 \times 10^6]\ A.m{-}2$
h	$[50000, 65000]\ W.m^{-2}.K^{-1}$
T_w	$[293, 313]\ K$

Table 6: Input parameters ranges

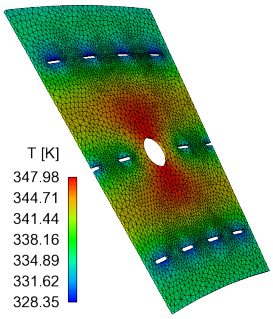

Fig. 2: Temperature

Performed in parallel on 8 processors, the results given hereafter are based on a set of 1000 realizations for which parameters are randomly chosen in the ranges of table 6. The non-linearity is handled by a fixed point iterative method, but this time with a Picard algorithm instead of a Newton method. Nevertheless, all previous considerations apply in the same way. As for the benchmark, we display the maximum of absolute errors (16) on solution and on output to be compared with reference results obtained with the standard method. The considered EIM trainset is of size 100.

The first tables 7a and 7b compare the SER1 method with the standard one, both based on a randomly selection process to build the RB approximation space.

N	M	$max(\varepsilon^u_{M,N})$	$max(\varepsilon^s_{M,N})$
5	5	1.64e+1	1.94e-1
10	10	6.84e+0	8.24e-2
15	15	6.30e-2	4.90e-4
20	20	1.31e-2	1.65e-4
25	25	9.80e-3	6.74e-5

(a) Standard - RB random

N	M	$max(\varepsilon^u_{M,N})$	$max(\varepsilon^s_{M,N})$
5	5	1.05e+1	2.09e-2
10	10	5.07e-1	3.42e-3
15	15	5.24e-1	1.05e-3
20	20	9.23e-2	1.89e-4
25	25	3.26e-2	1.90e-4

(b) SER(1) - RB random

Turning to the previously introduced error estimator, the table 8 displays the errors obtained from its use into the parameter selection process. Besides its low impact on the 2D benchmark illustrated by the tables 2a and 2b, the Greedy algorithm used to build the RB approximation space has a significant influence on this application. Indeed, it results in errors whose order of magnitude comes close to ones obtained with standard RB methodology.

N	M	$max(\varepsilon^u_{M,N})$	$max(\varepsilon^s_{M,N})$
5	5	7.66e+0	2.71e-2
10	10	3.37e-1	7.82e-4
15	15	4.85e-2	2.64e-4
20	20	2.93e-2	3.40e-4
25	25	5.23e-3	4.59e-5

Table 8: SER(1) - RB Greedy

The convergence study of the SER(1) method and its variants on this kind of application allows to go further in its analysis. To this purpose, the figure 3a focuses on the convergence study related with the EIM approximation considered for the electrical conductivity $\sigma(T)$. Besides the expected error decrease, this plot highlights the enhancement coming from the use of the error indicator in term of convergence. The figure 3b studies the relative L_2 error of the RB approximation depending on the number of basis functions. The resulting behaviour was expected as well.

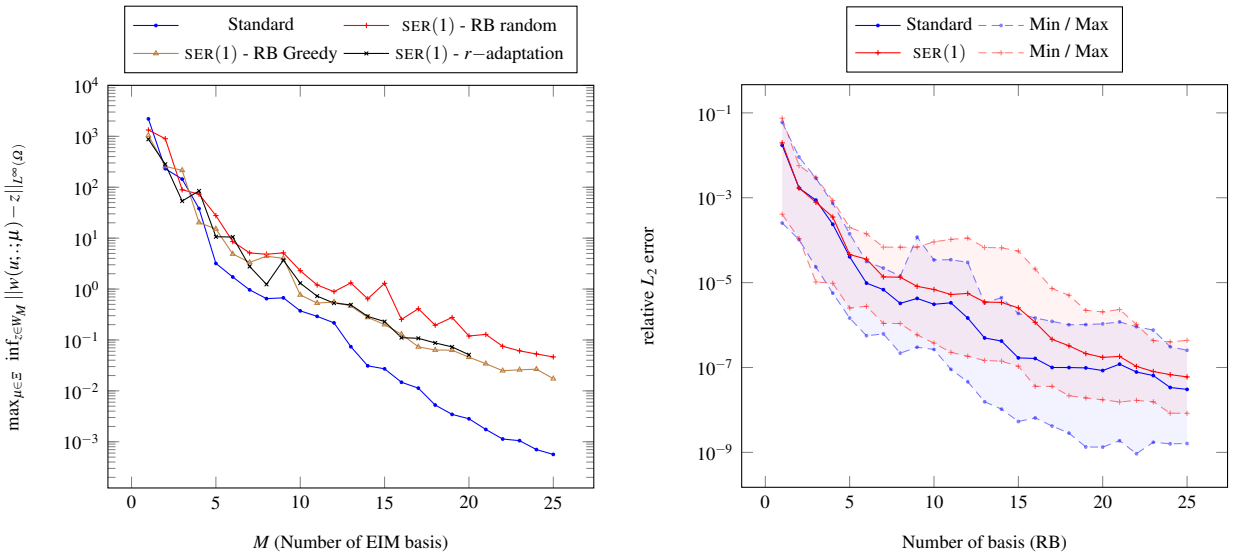

(a) EIM approximation of $\sigma(T)$

(b) Reduced basis solution

Fig. 3: SER method - EIM and RB convergence

Regarding its impact on the previous 2D benchmark, we investigate as well the use of multilevel SER(ℓ) method with $l \geqslant 1$ on the electro-thermal problem. In this context, the table 9 compares the results obtained at first and second levels. In spite of the random selection process, the table 9a is in good agreement with the previous table 7b. The table 9b confirms the relevance of the multilevel variant since SER(2) already gives results which come close to those obtained with standard RB methodology.

N	M	$\max(\varepsilon^u_{M,N})$	$\max(\varepsilon^s_{M,N})$
5	5	2.56e+1	2.85e-1
10	10	9.55e+0	6.06e-2

(a) SER(1)

N	M	$\max(\varepsilon^u_{M,N})$	$\max(\varepsilon^s_{M,N})$
5	5	7.78e+0	3.57e-2
10	10	2.09e+0	4.92e-3

(b) SER(2)

Table 9: SER multilevel - Random

As for the figure 1 in the case of the 2D benchmark, the convergence study of the considered EIM approximations allows to go further in the analysis. To this end, the figure 4a (resp. 4b) compares the convergence resulting obtained from various level for the EIM approximation of $\sigma(T)$ (resp. $k(T)$). This study tends to confirm the preliminar results obtained on the benchmark which show pertinence of this SER variant.

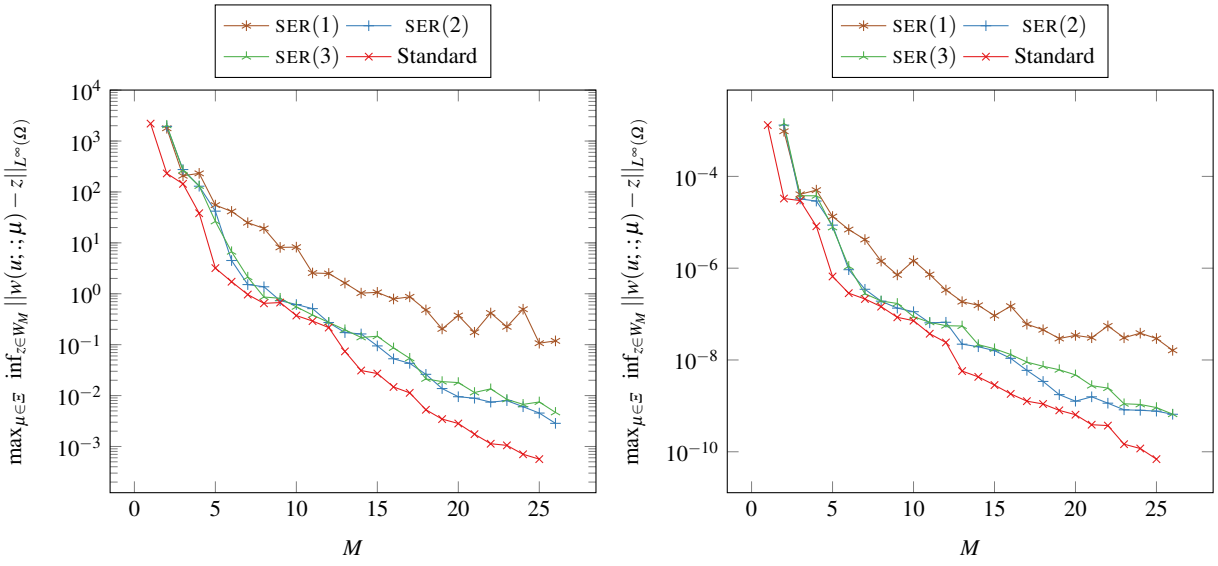

(a) EIM $\sigma(T)$

(b) EIM $k(T)$

Fig. 4: SER multilevel - Random - EIM convergence

4.3 Application to Polyhelix magnet

As an alternative of the previously mentionned Bitter magnets, the polyHelix are designed to produce high magnetic fields. Detailled in [2], this technology rests on complex geometries leading to large problems in a numerical point of view. The saving in computational time offered by the SER method is thus all the more pertinent in this context. We propose to investigate its use on such a problem.

Based on a mesh composed of 2.2 millions of tetrahedra for approximatively 500000 nodes (figure 5), the next simulations are performed on 12 processors. The computer used to perform this experiment is composed of 2 multi-threaded 6 cores CPUs and 141 GB of shared memory. The considered problem is similar to the one introduced in (17) for the Bitter magnet. The underlying non-linearity is handled by a Picard method with a given tolerance of 10^{-6}. Except the parameter related with the current flow, the input data are similar to the previous experiment. The current density previously considered is this time replaced by the difference of potential V_D which directly gives the Dirichlet boundary condition (19).

Input	Range
σ_0	$[50\times10^6, 50.2\times10^6]\ S.m^{-1}$
α	$[3.3\times10^{-3}, 3.5\times10^{-3}]\ K^{-1}$
L	$[2.5\times10^{-8}, 2.9\times10^{-8}]$
V_D	$[55, 65]\ V$
h	$[70000, 90000]\ W.m^{-2}.K^{-1}$
T_w	$[293, 313]\ K$

Table 10: Input parameters ranges

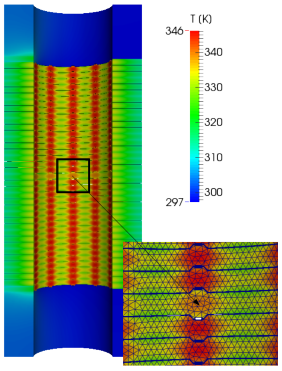

Fig. 5: Temperature

The next study is based on EIM and RB approximation spaces of size 5. It aims to compare the computational time necessary to perform the EIM Greedy algorithm with the standard RB methodology and with the introduced SER method. To this end, we focus on the EIM approximation related with the electrical conductivity $\sigma(T)$ for which the considered trainset is composed of 100 parameters.

Consisting of the same finite element solve in both cases, the computational time related with the initialization of the EIM building step is approximatively 1760 seconds. The SER method uses the reduced basis approximation which results from the first EIM basis function while the standard methodology continue to use finite elements approximations. Regarding the first EIM Greedy algorithm for which the available reduced basis approximation rests on a single basis function, the mean time required to solve the reduced problem is 2.1 seconds compared with 2087 seconds for the corresponding finite element one. Regarding the whole set of resolutions performed within the EIM Greedy algorithm, this amounts to a factor close to 500 in terms of computational time.

Through each stage of the SER method, the EIM basis functions are built from a set of reduced basis approximations based on an enriched RB approximation space. In this context, the table 11 displays the mean time necessary for a single resolution and the resulting gain factor related with the whole EIM Greedy algorithm.

N	Mean time per online realization (s)	Gain factor observed for EIM Greedy algorithm
1	2.1	495
2	4.3	321
3	7.7	213
4	6.1	254

Table 11: Performances of the SER method on a large scale multi-physics problem

Still considering the mean temperature over the domain, the use of the standard methodology with $N = M = 5$ results in an maximal output error of 4.5×10^{-2}. Only the SER method combined with the error indicator ensures the convergence of the online stage which itself results in a maximal error of 2.1×10^{-1} compared with the finite element approximation. As to the initial SER method using a random selection process regarding the building of the RB approximation space, it has convergence issues for some input parameters. It illustrates the relevance of a smart selection process, — the error indicator.

5 Conclusion

Intended as a follow-up of [1] introducing the SER method, this paper investigates some of its variants and in particular SER(ℓ) as well as the benefits of using an error indicator to drive the SER process. We have proposed a methodology that can build simultaneously the affine decomposition of the original problem and the associated reduced basis model. Both (EIM and RB) are feeding each other. We recover convincing error convergence on EIM and RB on a standard benchmark problem as well as on 3D industrial nonlinear multi-physics application. There are still various aspects of the methodology that can be investigated, we believe that SER opens various opportunities, and there is of course the theoretical question of the a priori convergence of the SER method — the methodology takes advantage of the underlying low-dimensional structures of the nonlinear PDE systems simultaneously from the EIM and RB sides.

Acknowledgements

The authors would like to thank A.T. Patera (MIT) for the fruitful discussions we had as well as Vincent Chabannes (U. Strasbourg) and Christophe Trophime (CNRS). The authors acknowledge also the financial support of the ANR Chorus and the Labex IRMIA.

References

1. Daversin, C., Prud'homme, C. : Simultaneous empirical interpolation and reduced basis method for non-linear problems. C. R. Acad. Sci. Paris, Ser. I **353**, 1105–1109 (2015)
2. Daversin, C., Prud'homme, C., Trophime, C. : Full Three-Dimensional Multiphysics Model of High-Field Polyhelices Magnets. IEEE transactions on applied superconductivity **26(4)** (2016)
3. Grepl M.A., Maday Y., Nguyen, N.C. Patera, A.T. : Efficient reduced-basis treatment of nonaffine and nonlinear partial differential equations. Modél. Math. Anal. Numér. **41(03)**, 575–605 (2007)
4. Barrault, M., Maday, Y., Nguyen, N.C., Patera, A.T. : An empirical interpolation method: application to efficient reduced-basis discretization of partial differential equations. C. R. Acad. Sci. Paris, Ser. I **339(9)**, 667–672 (2004)
5. Daversin, C., Veys, S., Trophime, C., Prud'homme, C. : A Reduced Basis Framework: Application to large scale non-linear multi-physics problems. ESAIM Proc. EDP Sciences Paris **43**, 225–254 (2013)
6. Veroy, K., Prud'homme, C., Rovas, D.V, Patera, A.T. : A Posteriori Error Bounds for Reduced-Basis Approximation of Parametrized Noncoercive and Nonlinear Elliptic Partial Differential Equations. American Institute of Aeronautics and Astronautics Paper, 2003-3847 (2003)